Macromolecules
ARTICLE

Macromolecules **2010**, *43*, 4771–4781 **4771**
DOI: 10.1021/ma902658n

Synthesis and Micellization of pH/Temperature-Responsive Double-Hydrophilic Diblock Copolymers Polyphosphoester-*block*-poly[2-(dimethylamino)ethyl methacrylate] Prepared via ROP and ATRP

Xu Liu, Peihong Ni,* Jinlin He, and Mingzu Zhang

Key Laboratory of Organic Chemistry of Jiangsu Province, College of Chemistry, Chemical Engineering and Materials Science, Soochow University, Suzhou 215123, China

Received December 1, 2009; Revised Manuscript Received March 12, 2010

ABSTRACT: Novel pH- and temperature-responsive double-hydrophilic diblock copolymers, poly(ethylethylene phosphate)-*block*-poly[2-(dimethylamino)ethyl methacrylate] (PEEP-*b*-PDMAEMA), have been synthesized via the combination of ring-opening polymerization (ROP) and atom transfer radical polymerization (ATRP). The PEEP block with a bromine-terminated end (PEEP-Br) was first prepared by ROP of 2-ethoxy-2-oxo-1,3,2-dioxaphospholane (EEP) using 2-hydroxyethyl 2-bromoisobutyrate as a bifunctional initiator and stannous octoate as a catalyst. ATRP was then used to polymerize DMAEMA monomer in a methanol/water mixture with PEEP-Br as a macroinitiator, resulting in diblock copolymers of PEEP-*b*-PDMAEMA. Their chemical structures were respectively characterized by ^{1}H NMR, ^{13}C NMR, ^{31}P NMR, and FT-IR. Their molar mass distributions were determined by gel permeation chromatography (GPC). The critical aggregation concentration (cac) of PEEP-*b*-PDMAEMA in aqueous solution, which was measured by the fluorescence probe technique, depends on the block composition. The results measured by static laser light scattering (LLS), dynamic light scattering (DLS), and transmission electron microscopy (TEM) reveal that these diblock copolymers are able to self-assemble into aggregates with different particle sizes and morphologies in aqueous solutions, depending on various pH media. On the other hand, the UV−vis measurement shows that these diblock copolymers exhibit a reproducible temperature-responsive behavior with a lower critical solution temperature (LCST) that is tunable by the block composition and pH. In addition, agarose gel retardation assays, TEM, and zeta potential measurements demonstrate that such double-hydrophilic diblock copolymers can effectively condense DNA, potentially useful for the gene delivery.

Introduction

Double-hydrophilic block copolymers (DHBCs)[1] represent a class of copolymers with two or more water-soluble blocks made of different chemical species. They exhibit switchable amphiphilic characteristics.[2] That is, one hydrophilic segment undergoes physical or chemical transformations and becomes hydrophobic, whereas another hydrophilic segment remains soluble in water. And the transformation is often induced by subtle adjustment of temperature, pH, or ionic strength in solutions as well as complexation with appropriate molecules. Thus, DHBCs provide a wide range of applications including drug delivery and gene therapy,[3,4] reversible solution condition-induced micellization,[5] crystal growth modifiers,[6] mineralization templates,[7] nanoparticle fabrication,[8,9] and so on. It is believed that more applications in biomedical field will be developed due to their stimuli responsiveness and easily tunable functionality. The nature of the monomer repeat units in each hydrophilic block can be either ionic or non-ionized. Typical ionic segments include poly(acrylic acid) (PAA), poly(styrenesulfonic acid) (PSSA), poly[2-(dimethylamino)ethyl methacrylate] (PDMAEMA), and poly(4-vinylpyridine) (P4VP).[1] However, most of DHBCs with nonionic block prepared so far are based on hydrophilic poly(ethylene oxide) (PEO) and its derivants.[10,11] Therefore, it is necessary to diversify systematically the nonionic hydrophilic block of DHBCs. The aim is to extend the types of double-hydrophilic block copolymers and to expect unique properties of their micelles in aqueous media.

*To whom correspondence should be addressed. E-mail: phni@suda.edu.cn.

In addition, for biomedical applications, biodegradability and biocompatibility would be a desirable trait of DHBCs. However, extensive design of biodegradable DHBCs has not been performed yet. The main limitation lies in the nondegradability of carbon−carbon backbone or ether-based backbone,[12] although it may be partially overcome by advanced polymer synthesis techniques. For example, a degradable block copolymer consisting of poly(ethylene glycol) (PEG) and PDMAEMA segments connected through an acid-labile cyclic ortho ester linkage (PEG-*a*-PDMAEMA) was synthesized by ATRP for gene delivery.[13]

Polyphosphoesters (PPE) have been pursued as biomaterials due to their potential biodegradability, good biocompatibility, and functionality of side chain[14] as well as their structural similarities to naturally occurring nucleic and teichoic acids. Interestingly, they can degrade under the physiological conditions via hydrolysis or enzymatic cleavage of the phosphoester bonds.[15,16] The degradation rates are controllable by adjusting the chemical structure in the backbone and side chain. By choosing biocompatible building blocks of the polymer, degradation products of PPE have minimal toxic effects and good biocompatibility.[17] As a result, polyphosphates have been proposed for use in many biomedical applications, ranging from drug and nonviral gene carriers[18] to cell encapsulations[19] and tissue engineering scaffolds.[20] Recently, polyphosphoesters (PPE) have been reported to be used in amphiphilic polymers as a hydrophilic block to replace traditional PEO. For example, Leong et al. synthesized random copolymers of poly(DL-lactide) (PLA) and poly(ethylethylene phosphate) (PEEP) as drug carrier and found that the hydrophilicity of the copolymers increased with the increasing EEP content.[21] Wang et al. reported the synthesis and degradation of

Published on Web 04/26/2010

Scheme 1. Synthesis Route of Double-Hydrophilic PEEP-*b*-PDMAEMA Diblock Copolymer

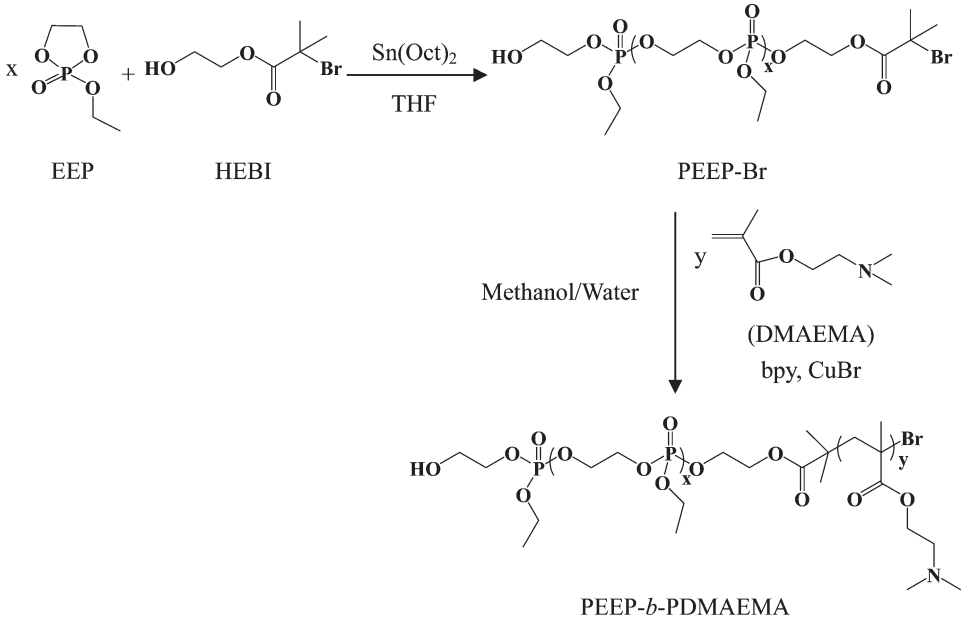

PEEP−PLLA−PEEP triblock copolymers, in which PLLA represents poly(L-lactic acid).[22] They have also widely researched the synthesis and application of amphiphilic block copolymers of PEEP and poly(ε-caprolactone) (PCL) as drug carrier.[23] Meanwhile, Iwasaki et al. recently reported that PEEP and its copolymers with poly(isopropylethylene phosphate) (P*i*PEP) are thermosensitive, exhibiting varied LCSTs, depending on the compositions.[24] Wang et al. also demonstrated that triblock copolymers of PEG, PEEP, and P*i*PEP exhibited thermo-induced self-assembly behavior, and their critical aggregation temperature can be conveniently adjusted.[25]

In this work, we have synthesized a series of diblock copolymers consisting of PEEP and PDMAEMA with various molecular weights and compositions through a combination of ring-opening polymerization (ROP) and ATRP strategy, as shown in Scheme 1. PDMAEMA has both pH- and temperature-sensitive behaviors in aqueous solutions, which acts as a weak polybase with pK_a of about 8.0.[26,27] In acidic or neutral media, PDMAEMA can be completely or partially protonated and has been reported to be one of the efficient condensing agents for DNA delivery. Nevertheless, low biodegradability limits its application in gene delivery.[28] Thus, focusing on the development of biodegradable DHBCs with both pH and temperature sensitivity for potential biomedical utility, we have synthesized PEEP-*b*-PDMAEMA diblock copolymers combining the advantages of polyphosphoester and PDMAEMA together. The effects of pH and temperature on the micellization under different conditions have been investigated. To the best of our knowledge, these PEEP-*b*-PDMAEMA diblock copolymers have not been reported previously. And we further demonstrated their potential application for gene delivery.

Experimental Section

Materials. 2-Ethoxy-2-oxo-1,3,2-dioxaphospholane (EEP) was synthesized by a method described previously[29] and distilled under reduced pressure just before use. 2-(Dimethylamino)ethyl methacrylate (DMAEMA, Aldrich) was dried over calcium hydride (CaH_2) and distilled in vacuum immediately before use. Stannous octoate [$Sn(Oct)_2$], 2,2′-bipyridine (bpy), 2-bromoisobutyryl bromide, and cuprous bromide (CuBr) were all purchased from Aldrich and used without further purification. THF was initially dried over potassium hydroxide for at least 2 days and then refluxed over sodium wire with benzophenone as an indicator until the color turned to purple. Ethidium bromide (EtBr) obtained from Fluka were used as received. Phosphate buffers saline tablets (PBS) and tris-borate-EDTA buffer (TBE) were obtained from Medicago. Plasmid pUC18 (pDNA) was purchased from Takara. Other reagents were purchased from Sinopharm Chemical Reagent Co. and used as received.

Synthesis of 2-Hydroxyethyl 2-Bromoisobutyrate (HEBI). HEBI was synthesized by a method described previously.[30] 2-Bromoisobutyryl bromide (4.998 g, 0.0218 mol) was added dropwise to a cold solution of ethylene glycol (30.759 g, 0.4961 mol) and triethylamine (2.202 g, 0.0218 mol) at 0 °C for 2 h. The reaction was continued at 0 °C for another 2 h and then heated to 40 °C for 5 h. The reaction mixture was cooled, added to 500 mL of water, and extracted with chloroform three times, and then the chloroform layer was washed successively with diluted HCl, saturated $NaHCO_3$, and water. The organic layer was dried over anhydrous magnesium sulfate and evaporated to provide a product. The product was vacuum-distilled (yield: 70%) and characterized with ^{1}H NMR (in $CDCl_3$): (CH_3)$_2$ CBr− (δ 1.80; 6H), −CH_2−CH_2−OH (δ 3.70; 2H), and −CH_2−CH_2−OH (δ 4.15; 2H).

Synthesis of PEEP-Br Macroinitiator. Polyphosphoester end-capped with bromo group (PEEP-Br) was prepared by ring-opening polymerization (ROP) of 2-ethoxy-2-oxo-1,3,2-dioxaphospholane (EEP) using HEBI as an initiator and $Sn(Oct)_2$ as a catalyst. The polymerization was conducted in a 50 mL round-bottom flask. The flask was treated with trimethylchlorosilane solution in methylene chloride for 12 h and flame-dried under vacuum, and three exhausting−refilling argon cycles were performed before use. A typical experimental procedure for polymerization was as follows: EEP monomer (2.0 g, 13.2 mmol) was introduced into the flask using a syringe, followed by adding 10 mL of THF. The mixture was subsequently stirred in a bath at 35 °C. To this solution was added HEBI (0.139 g, 0.66 mmol in 1.3 mL of THF) through a syringe, followed rapidly by addition of $Sn(Oct)_2$ (0.134 g, 0.33 mmol in 0.66 mL of THF). The solution was deactivated with 1 mol L^{-1} acetic acid after 1 h and precipitated into an excess of diethyl ether. The precipitate was dried under vacuum until a constant weight at room temperature to obtain the product.

Synthesis of PEEP-*b*-PDMAEMA Diblock Copolymer. PEEP-*b*-PDMAEMA diblock copolymers were synthesized in a methanol/water mixture at 25 °C via ATRP using PEEP-Br as a macroinitiator in a tightly sealed 50 mL round-bottom flask under an

argon atmosphere. As an example, the flask was charged with a required amount of macroinitiator PEEP-Br (0.306 g, 0.09 mmol) and DMAEMA monomer (0.424 g, 2.7 mmol). The solvent of deoxygenated methanol/water (2/1 by volume ratio) mixture was added to make the PEEP-Br solution of 0.1 mol L^{-1}. Three exhausting−refilling argon cycles were performed to remove oxygen from the polymerization solution, and then the solution was purged with argon gas for 10 min. CuBr (0.013 g, 0.09 mmol) and 2,2′-bipyridine (bpy) (0.029 mg, 0.18 mmol) were added with a slow argon purge. The flask was sealed under an argon atmosphere and kept in a water bath at 25 °C. The reaction was terminated by adding THF with stirring, and the solution turned from brown to blue. The reaction mixture was then allowed to pass through a basic alumina column. After being concentrated in a rotary evaporator, it was poured into cold hexane to precipitate the polymer. Finally, the copolymer was dialyzed against deionized water for 2 days to remove the unreacted PEEP-Br macroinitiator with a cellulose tubular membrane (MWCO 5000), and then lyophilized. The lost weight as unreacted PEEP-Br macroinitiator was used to estimate the initiation efficiency of the PEEP-Br macroinitiator. The yield of PEEP-*b*-PDMAEMA copolymer was determined gravimetrically.

Characterizations. ^{1}H NMR, ^{13}C NMR, and ^{31}P NMR spectra were recorded on an INOVA-300 NMR spectrometer at room temperature with $CDCl_3$ as a solvent and TMS as an internal reference. FT-IR measurements were performed on a Nicolet AVATAR 360 Fourier transform infrared spectrometer using the KBr disk method. Relative molecular weights and molecular weight distributions of PEEP-Br polymers were measured by a gel permeation chromatography (GPC) system equipped with a Waters 1515 Isocratic HPLC pump, a Waters 2414 refractive index detector (RI), a Waters 2487 dual-wavelength absorbance detector, and a set of Waters Styragel columns (HR3, HR4, and HR5, 7.8 mm × 300 mm). GPC measurements were carried out at 35 °C using dimethylformamide (DMF) as eluent with a flow rate of 1.0 mL min^{-1}. The system was calibrated with polystyrene standards. While the molecular weights and molecular weight distributions of PEEP-*b*-PDMAEMA diblock copolymers were determined by a Waters 1515 GPC instrument using a PLgel 5.0 μm bead-size guard column (50 × 7.5 mm^2), followed by two linear PLgel columns (500 Å and Mixed-C) and a differential refractive index detector. THF was used as the eluent at 30 °C with a flow rate of 1.0 mL min^{-1} and a series of standard monodispersed polystyrene as the calibration.

The critical aggregation concentration (cac) was investigated by the fluorescence probe method. Fluorescence spectra were recorded on a FLS920 fluorescence spectrofluorometer (Edinburgh Co., UK), and pyrene was used as a hydrophobic fluorescent probe. A predetermined amount of pyrene in acetone was added into a series of ampules, and the acetone was allowed to evaporate. 10 mL of aqueous solutions at different concentrations of copolymers was then added to the ampules containing the pyrene residue. It should be noted that all the aqueous solutions contained excess pyrene residue at the same concentration of 6×10^{-7} M. All the solution pH was adjusted to 9.2 for the cac measurement. The aqueous solutions of copolymers were allowed to stir for 24 h at room temperature to reach the solubilization equilibrium of pyrene. Excitation was carried out at 335 nm, and emission spectra were recorded ranging from 350 to 500 nm. Both excitation and emission bandwidths were set at 1 nm. From the pyrene emission spectra, the intensity ratio (I_3/I_1) of the third band (383 nm, I_3) to the first band (372 nm, I_1) was analyzed as a function of polymer concentration. The cac value was defined as the point of intersection of the two lines in the plot of fluorescence versus concentration. The experiments were conducted in triplicate, and the average values are reported.

A commercial LLS spectrometer (ALV/SP-125) equipped with a multi-τ digital correlator (ALV-5000/E) and a 22 mW He−Ne laser (JDS-Uniphase 1145P) was used. The incident beam was vertically polarized with respect to the scattering plane. The details of LLS instrumentation and principles can be found elsewhere.[31] In static LLS, the scattering angle (θ) and polymer concentration (C, g/mL) dependence of the absolute time-averaged scattered light intensity, known as the excess Rayleigh ratio ($R_{vv}(q)$), of a sufficiently dilute polymer solution can lead to the weight-averaged molar mass (M_w), the second virial coefficient (A_2), and the z-average mean-square radius of gyration $\langle R_g^2 \rangle$ as

$$\frac{KC}{R_{vv}(q)} \approx \frac{1}{M_w}\left[1 + \frac{1}{3}q^2\langle R_g^2\rangle\right] + 2A_2C \qquad (1)$$

where $K [= 4\pi n^2(dn/dC)^2/(N\lambda_0^4)]$ is a constant for a given polymer solution/dispersion and $q [= (4\pi n/\lambda_0)\sin(\theta/2)]$ is the scattering vector, with dn/dC, N_A, and λ_0 being the specific refractive index increment, the Avogadro number, and the light wavelength in vacuum, respectively. dn/dC was determined by using the Jianke differential refractometer.[32]

The particle sizes of the aggregates of PEEP-*b*-PDMAEMA diblock copolymer in aqueous solution were measured by a Zetasizer Nano-ZS dynamic light scattering instrument (Malvern) equipped with a 633 nm He−Ne laser using backscattering detection. All samples had a constant concentration of 2 g L^{-1}. The measurements were carried out at a scattering angle of 90° and at ambient temperature and various pH.

Transmission electron microscopy (TEM) images were obtained using a TEM instrument (TECNAI G^2 20, FEI Co.) in a 200 kV. To prepare the TEM samples, 5 μL of the sample solution was dropped onto a carbon-coated copper grid (400 meshes), and the water droplet was allowed to evaporate slowly in air.

The thermoresponsive properties of PEEP-*b*-PDMAEMA diblock copolymers were investigated with a Shimadzu 3150 UV−vis−NIR spectrophotometer. PEEP-*b*-PDMAEMA samples were dissolved in deionized water (0.5 wt %), and a transmittance curve through the solution at a wavelength of 500 nm was recorded with temperature variation (0.1 °C min^{-1}) between 30 and 80 °C. The lower critical solution temperature (LCST) of the polymer solution was defined as the temperature producing a half decrease of the total decrease in optical transmittance.

The ability of compacting DNA for PEEP-*b*-PDMAEMA diblock copolymer was investigated by several methods, including gel retardation assay, zeta potential measurements, and TEM. For gel retardation assay, polyplexes in different N/P ratios were loaded onto 0.8% agarose gel containing ethidium bromide (0.5 μg mL^{-1}) and then electrophoresed in Tris-borate-EDTA buffer (TBE: 40 mM tris-borate, 1 mM EDTA, and pH 7.4) at 70 V for 1 h. The migrated pDNA was visualized on a UV illuminator (M-15E, UVP Inc., Upland, CA), and the determination of aqueous microelectrophoresis of pDNA/PEEP-*b*-PDMAEMA complexes was carried out in a JS94J microeletrophoresis instrument (Shanghai Zhongchen Co., China). The device used a CCD camera, frame grabber, and software to capture the image of the moving particles. The zeta potential data were directly calculated by the instrument. The morphologies of pDNA and pDNA/PEEP-*b*-PDMAEMA complexes were observed by TEM.

Results and Discussion

Synthesis and Characterization of the Diblock Copolymers. The synthetic route for the preparation of PEEP-*b*-PDMAEMA diblock copolymer is outlined in Scheme 1. As reported by Jakubowski et al., ring-opening polymerization (ROP) can be hindered in the presence of DMAEMA because the complexation of the amine site of PDMAEMA would deactivate tin(II) hexanoate, which was used as a catalyst for ROP.[30] Therefore, in the present work, DMAEMA monomer was polymerized following PEEP block. PEEP-Br with linear molecular structure was synthesized through ring-opening polymerization of EEP in THF under co-initiation of difunctional ATRP/ROP initiator 2-hydroxyethyl 2-bromoisobutyrate (HEBI) and $Sn(Oct)_2$. The feed molar ratio of HEBI to

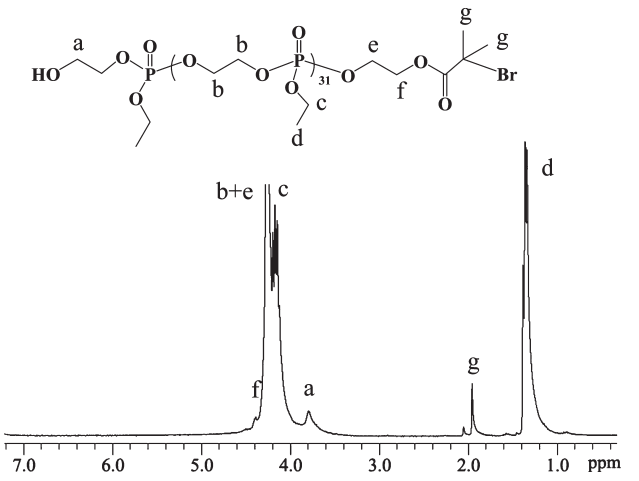

Figure 1. ^{1}H NMR spectrum of the bromine-terminated polyphosphoester ($PEEP_{32}$-Br) (solvent: $CDCl_3$).

EEP was 1:30, while the reaction time was limited to 1 h since the extension of reaction time will likely lead to chain exchange side reaction though EEP conversion can be increased.[33] PEEP-*b*-PDMAEMA diblock copolymer with controlled molecular weight and low polydispersity was then prepared by ATRP technique. A CuBr/bpy catalyst system was used for the polymerization of DMAEMA using PEEP-Br as a macroinitiator in a methanol/water mixture according to previous literature.[34] The obtained diblock copolymer PEEP-*b*-PDMAEMA was characterized by NMR as described in the Experimental Section.

Figure 1 shows the ^{1}H NMR spectrum of PEEP-Br. Resonances at δ 1.37 ppm (peak d), δ 4.18 ppm (peak c), and δ 4.26 ppm (peak b + e) are assigned respectively to pendent methyl [$-$P(=O)$-$OCH$_2$CH_3], methylene [$-$P(=O)$-$OCH_2-CH$_3$] protons, and methylene protons [$-$P(=O)$-$OCH_2-CH_2O$-$] from PEEP backbone. And the resonance at δ 3.81 ppm (peak a) should be assigned to the methylene protons conjoint to the end hydroxyl group of phosphoester unit of block copolymer [$-$P(=O)$-$OCH$_2$CH_2OH]. From the resonances of protons for initiator HEBI [δ 1.80 ppm; (CH_3)$_2-$CBr$-$] appearing in Figure 1, one can observe that HEBI had been involved in the ring-opening polymerization of EEP. The typical ^{1}H NMR spectrum of diblock copolymer of PEEP-*b*-PDMAEMA is shown in Figure 2A. It is found that all signals assigned to protons of PEEP block (except for the terminal methyl directly linked to the bromine group) in Figure 1 are also present in the spectrum of PEEP-*b*-PDMAEMA diblock copolymer. Those newly appearing signals in Figure 2A are assigned as δ 0.7$-$1.3 ppm for the α-CH_3 (peak f), δ 1.9 ppm for the protons in $-$CCH_2- (peak e), δ 2.3 ppm for the protons in $-$N(CH_3)$_2$ (peak i), δ 2.6 ppm for the $-$CH_2N= (peak h), and δ 4.1 ppm for the methylene neighboring to the ester group [$-C\mathit{H}_2$OC(=O)] (peak g) of the PDMAEMA block. The ^{13}C NMR spectrum also revealed that resonances of carbon atoms from the PEEP and the PDMAEMA block were all presented as assigned in Figure 2B.

The ^{31}P NMR spectrum of PEEP-*b*-PDMAEMA diblock polymer (Figure 2C) gave a strong resonance at δ $-$0.25 ppm (peak b), assigned to the phosphorus atoms in polyphosphoester block except the phosphorus atom at the end, which generated the weak signal at δ 0.6 ppm (peak a).

FT-IR analysis results of PEEP homopolymer and PEEP-*b*-PDMAEMA diblock polymer are shown in Figure 3. Absorption (bands) at 1276 and 1158 cm^{-1} in Figure 3a can be observed, which can be ascribed to the asymmetrical and symmetrical P=O stretching, respectively. The P$-$O$-$C stretching

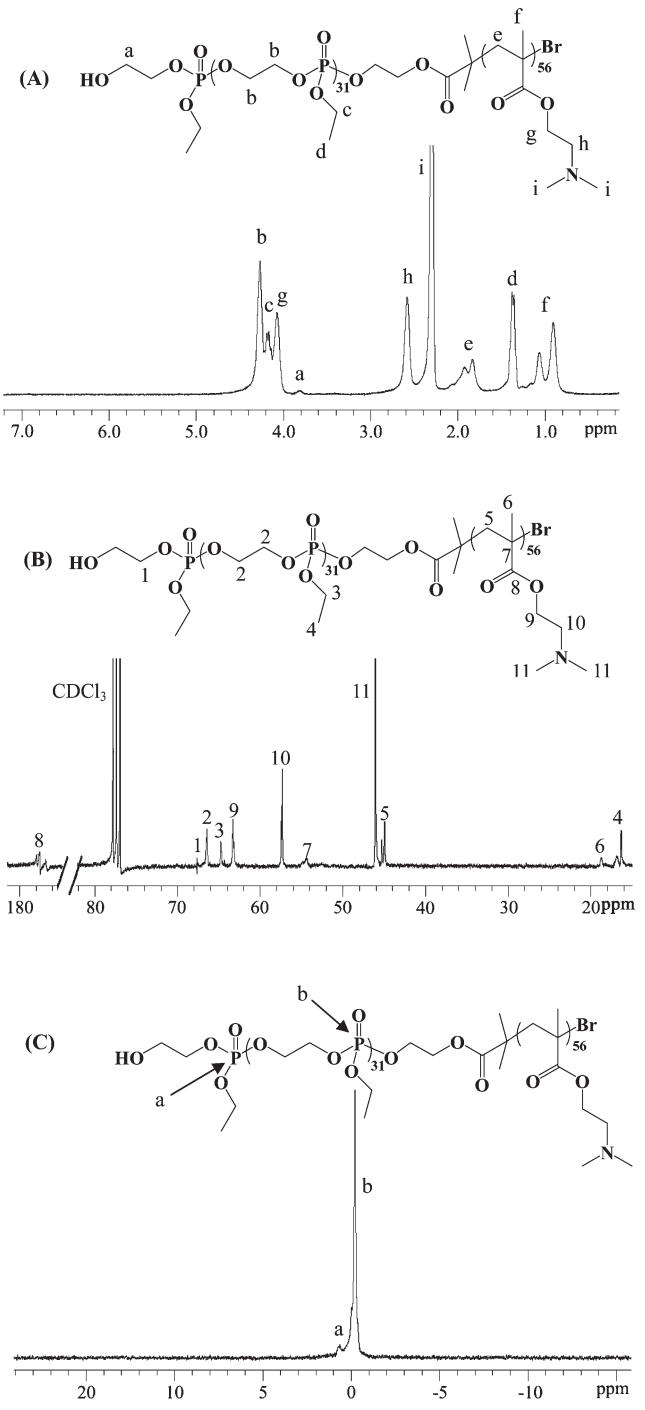

Figure 2. Typical characterization of NMR spectroscopy for $PEEP_{32}$-*b*-$PDMAEMA_{56}$ diblock copolymers: (A) ^{1}H NMR, (B) ^{13}C NMR, and (C) ^{31}P NMR. $CDCl_3$ was used as the solvent in each measurement.

is also verified at 988 cm^{-1} in the FT-IR spectrum. According to the FT-IR spectrum shown in Figure 3b, the following characteristic peaks of PDMAEMA can be found: 1735 cm^{-1}, carbonyl (C=O) stretch vibration; 2920$-$2960 cm^{-1}, $-$N(CH$_3$)$_2$ stretch vibration; around 1476 cm^{-1}, $-$N(CH$_3$)$_2$ deformational stretch vibration. Those absorptions, however, are absent in the FT-IR spectrum of PEEP homopolymer. Thus, judging together with analysis by NMR spectrum, it demonstrated the successful polymerization of diblock copolymer PEEP-*b*-PDMAEMA.

The number-average molecular weights ($\bar{M}_n$) and polydispersity indexes (PDI) of PEEP-Br homopolymers and

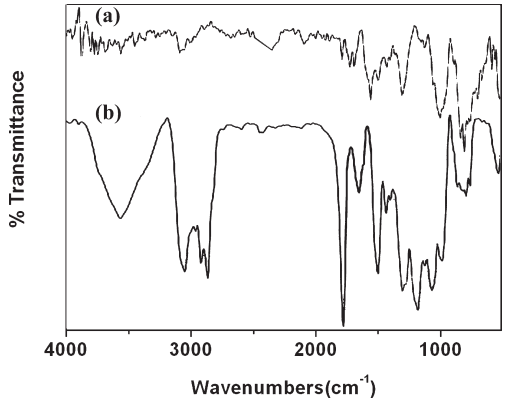

Figure 3. FT-IR spectra of (a) $PEEP_{32}$-Br macroinitiator and (b) $PEEP_{32}$-*b*-$PDMAEMA_{56}$ diblock copolymer.

PEEP-*b*-PDMAEMA diblock copolymers were measured by GPC. For both, we tried to perform GPC measurement using DMF and THF as eluents. Unfortunately, signals of PEEP homopolymers were only detected in DMF (refractive index: 1.4305) and PEEP-*b*-PDMAEMA in THF (refractive index: 1.4040). The reason lies in the difference of refractive index of polymers and eluents. Although GPC analysis based on linear polystyrene standards is not a reliable approach to determining the accurate molecular weights of polyphosphoester, it is meaningful in estimating the PDI values. The molecular weight distribution for PEEP-Br was narrow. The actual molecular weights of PEEP-Br was calculated according to the relative integration intensities of methylene protons of PEEP-Br (peak b of ^{1}H NMR spectrum in Figure 1) and the protons from HEBI group at one end of the polymer chain (peak g in Figure 1). The molar masses of the copolymers were calculated by comparing the intensity of the methylene protons (peak h of ^{1}H NMR spectrum, Figure 2A) of PDMAEMA at 2.6 ppm with the methyl protons of PEEP at δ 1.37 ppm (peak d, Figure 2A). Detailed information on the PEEP-Br homopolymers and PEEP-*b*-PDMAEMA diblock copolymers has been summarized in Table 1. It can be seen that the $\bar{M}_{n,NMR}$ values of the diblock copolymers as calculated by the ^{1}H NMR spectrum are slightly higher than the theoretical ones. The actual initiation efficiency was about 90%. This is owing to the high molecular weight of PEEP macroinitiator, which leads to high viscosity of the reaction solution and enhanced embedment of the radicals at the chain ends with long PEEP chains. Meanwhile, PDMAEMA-containing polymers are difficult to be characterized by GPC because of the adsorption of PDMAEMA block onto the column.[35] This usually results in broader peaks (larger polydispersities) with higher retention times (lower molecular weights).

Critical Aggregation Concentration (cac). The cac value of a diblock copolymer is an important parameter that represents the self-assembling behavior of block copolymers in solution. In this study, the fluorescence probe method was used to determine the cac value of PEEP-*b*-PDMAEMA copolymers, and all the solution pH was adjusted to 9.2 to reach a complete deprotonation. Pyrene is a common probe used to monitor micropolarity because the ratio of the third to the first vibronic peaks (I_3/I_1) in pyrene fluorescence spectrum is sensitive to the polarity, the I_3/I_1 ratio being larger in less polar media.[36] And I_3/I_1 ratio variations with polymer concentrations can be monitored. The cac values were plotted against the degrees of polymerization (DPs) of both PDMAEMA and PEEP blocks in the diblock copolymers and shown in Figure 4. When the DP of PEEP block increased from 21 to 32, while the DP of PDMAEMA was fixed at 31, the cac values increased from 0.74 to 0.91 g L^{-1}. This trend is in agreement with the reported result by Wang et al., in which a block copolymer with a rather long PEEP segment tended to increase the cac value in aqueous media.[23b] When the DP of PEEP was fixed at 32, but the DP of PDMAEMA was varied from 31 to 67 units, the cac value decreased from 0.91 to 0.86 g L^{-1}, indicating that the length of PDMAEMA block plays an important role on the thermodynamic stability of micelles. Compared with PEG, the PEEP block is slightly hydrophobic. Therefore, we can believe that PEEP-*b*-PDMAEMA micelles would be more thermodynamically stable in aqueous media. In this sense, PEEP-*b*-PDMAEMA micelles should be a potential candidate for biomedical application.

Table 1. Characterization Data of the Compositions, Number-Average Molecular Weights, and Molecular Weight Distributions of PEEP Macroinitiators and PEEP-*b*-PDMAEMA Diblock Copolymers

sample	$\bar{M}_{n,GPC}$	$\bar{M}_{n,theor}$[c]	$\bar{M}_{n,NMR}$[d]	PDI[e]
$PEEP_{21}$	7340[a]	3690	3400	1.13
$PEEP_{21}$-*b*-$PDMAEMA_{31}$	7840[b]	8260	9400	1.41
$PEEP_{21}$-*b*-$PDMAEMA_{43}$	9280[b]	10140	10860	1.24
$PEEP_{21}$-*b*-$PDMAEMA_{45}$	12280[b]	10390	10590	1.30
$PEEP_{26}$	9320[a]	4450	4150	1.21
$PEEP_{26}$-*b*-$PDMAEMA_{20}$	4400[b]	6560	7290	1.23
$PEEP_{32}$	12200[a]	5440	5130	1.19
$PEEP_{32}$-*b*-$PDMAEMA_{31}$	6920[b]	10000	11470	1.29
$PEEP_{32}$-*b*-$PDMAEMA_{40}$	8110[b]	11410	14270	1.39
$PEEP_{32}$-*b*-$PDMAEMA_{56}$	10450[b]	13920	14360	1.36
$PEEP_{32}$-*b*-$PDMAEMA_{67}$	11730[b]	15450	18320	1.33

[a] GPC in DMF/LiBr, using polystyrene as standards. [b] GPC in THF, using polystyrene as standards. [c] Theoretical molecular weight. [d] Calculated on the basis of ^{1}H NMR measurements in $CDCl_3$. [e] Measured by GPC in corresponding solvent.

pH-Responsive Properties of PEEP-*b*-PDMAEMA Diblock Copolymers. It is well-known that PDMAEMA possesses pH-responsive properties. Herein, we have investigated the effect of pH variation on the aggregation behavior of PEEP-*b*-PDMAEMA diblock copolymers by performing TEM and laser light scattering (LLS).

Figures 5 to 7 show TEM images of the micelles obtained by the self-assembly of $PEEP_{32}$-*b*-$PDMAEMA_{67}$ diblock copolymer in aqueous solution at pH 3.0, 7.4, and 9.5, respectively. All solution concentrations were kept at 2.0 g L^{-1}, which was above the cac of $PEEP_{32}$-*b*-$PDMAEMA_{67}$ solution. It is clear that the particle sizes of aggregates at pH 3.0 are larger than those at both pH 7.4 and 9.5, and with different morphologies, indicating that the diblock copolymer has pH-responsive properties. We have proposed possible aggregating structures to explain the above-mentioned phenomenon as shown in Scheme 2.

Under acidic conditions (pH 3.0), the PEEP-*b*-PDMAEMA diblock copolymers were expected to be individual unimers because both PEEP block and DMAEMA segments with sufficient protonation were hydrophilic. Tam et al. reported the unimer state of PEO-*b*-PDEAEMA in acidic solution.[37] In our test, however, aggregates were surprisingly observed as shown in Figure 5. It is because of the hydrolysis of PEEP segments. Penczek et al. explored the stability of the poly(alkylene phosphates) in aqueous solutions at various pH values and the relative rates of hydrolysis for the main chain and methyl substituent on phosphorus via direct titrimetric and NMR methods.[38] In acidic conditions the methyl group hydrolyzes faster, whereas at basic conditions both the methyl group and the main chain depart with approximately similar rates. This difference results from different mechanisms of

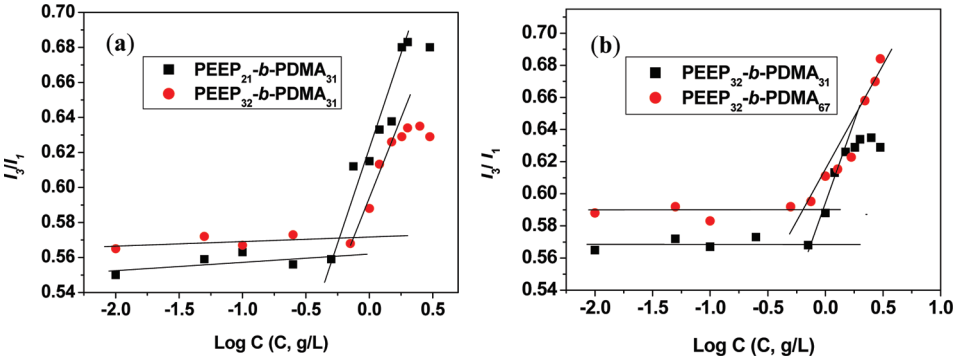

Figure 4. Intensity ratios (I_{383}/I_{372}) as a function of concentration of PEEP-*b*-PDMAEMA (PEEP-b-PDMA in short) with different degrees of polymerization for (a) changed PEEP length and (b) changed PDMAEMA length.

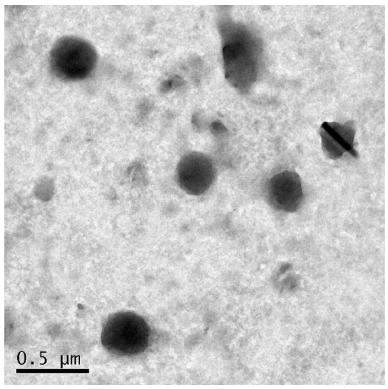

Figure 5. TEM micrographs of aggregates from $PEEP_{32}$-*b*-$PDMAEMA_{67}$ diblock copolymer in solution at pH 3.0 with a concentration of 2.0 g L^{-1}, bar = 0.5 μm.

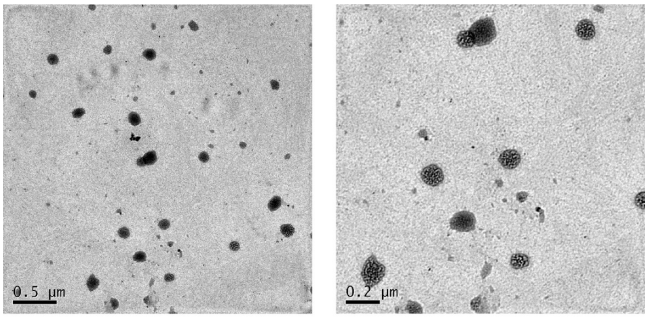

Figure 6. TEM micrographs of (a) aggregates from $PEEP_{32}$-*b*-$PDMAEMA_{67}$ diblock copolymer in solution at pH 7.4 with a concentration of 2.0 g L^{-1}, bar = 0.5 μm, and (b) the high-magnification image of (a), bar = 0.2 μm.

hydrolysis: in acidic conditions the carbon atoms are attacked (as indicated in Figure 8), whereas in basic conditions the phosphorus atom is attacked. The period breaking 1% of bonds in the macromolecule was about 150 h at pH 2.0 and 45 °C.

Furthermore, Wang et al. investigated the degradation of PEEP-*b*-PLA-*b*-PEEP block polymers at various pH.[22] They found that the M_w of PEEP-*b*-PLA-*b*-PEEP block polymers decreased from 13 740 to 9230 g mol^{-1} after 21 day in acidic conditions, demonstrating a slow degradation rate of PEEP chain.

As PEEP-*b*-PDMAEMA aqueous solutions with pH 3 were prepared from the original one (with pH 8.2) by adding hydrochloric acid solution and stirred overnight, it is not surprising

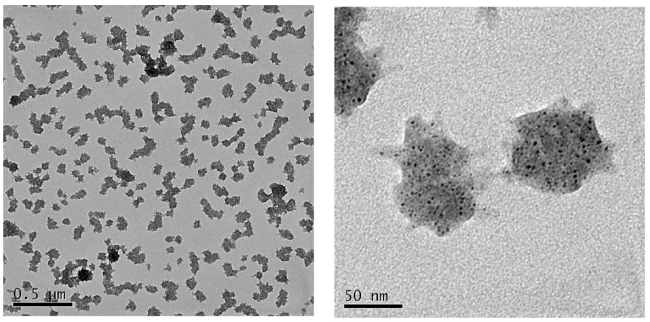

Figure 7. TEM micrographs of (a) aggregates from $PEEP_{32}$-*b*-$PDMAEMA_{67}$ diblock copolymer in solution at pH 9.5 with a concentration of 2.0 g L^{-1}, bar = 0.5 μm, and (b) the high-magnification image of (a), bar = 50 nm.

Scheme 2. Proposed Microstructure Transformation of the PEEP-*b*-PDMAEMA Diblock Copolymer at Different pH Values

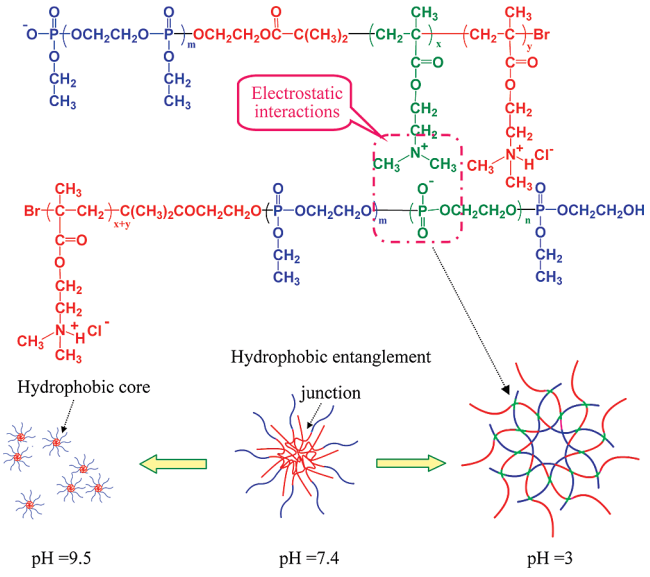

that a slight portion of the PEEP segments have been hydrolyzed, especially the ethyl group, resulting in an ionic block bearing negative charges. Wang et al. proved the hydrolytic products of PEEP at acidic condition, as shown in Figure 9. After hydrolysis, PEEP-*b*-PDMAEMA copolymer turned into polyampholyte species. Therefore, it is reasonable to assume that the aggregates arise mainly from electrostatic interactions between the partially negatively charged PEEP segments

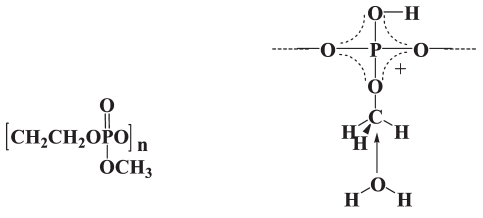

Figure 8. Chemical structure and its hydrolysis mechanism in acidic conditions.[38]

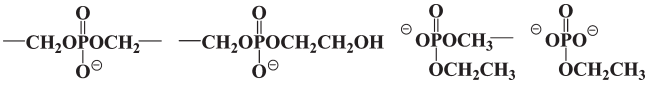

Figure 9. Degradation products of PEEP.[22]

and the positively charged PDMAEMA segments. A similar result has been reported by Tsitsilianis et al., who found a three-dimensional physical network formed in a limited pH range through electrostatic interactions between the few negatively charged PAA segments located in the end blocks and the positively charged P2VP segments located in the middle block of PAA_{134}-$P2VP_{628}$-PAA_{134}.[39]

On the other hand, the fact that particle size of the aggregates was much larger in acid solutions than those in neutral and basic solutions can be mainly attributed to the full protonation of the tertiary amine functional groups, which caused PEEP-*b*-PDMAEMA micelles to swell as the copolymer chains repel each other through electrostatic interactions.[40]

Under the condition of pH 7.4 in Scheme 2, the hydrolysis of PEEP segments is negligible because of the slow degradation rate and short time of stirring (12 h).[22] In this case, the repulsion effect of positive charges of protonated PDMAEMA block decreases, and partially deprotonated amine groups may produce pockets of hydrophobic segments that are randomly distributed along the PDMAEMA chains. Relatively small and loose aggregates are thus thought to be formed due to interchain entanglements and association of these short hydrophobic segments.

In basic conditions as shown in Scheme 2, the PDMAEMA block is fully deprotonated and becomes a hydrophobic chain, causing the PEEP-*b*-PDMAEMA diblock copolymer to become amphiphilic. Therefore, micelles are formed with the deprotonated PDMAEMA blocks as a hydrophobic core and the PEEP blocks as the hydrophilic corona. As described above, the degradation of PEEP could be accelerated in basic conditions and degradation rate of main chain was faster than that of ethyl groups, resulting in a series of negative charged PEEP-*b*-PDMAEMA chains with different degrees of degradation. Thus, large and loose aggregates formed with those different micelles together.

SLS and DLS analysis can also present evidence for the above explanations. The weight-average molar mass (M_w) of the aggregates at various pH were measured using the SLS technique via eq 1. Berry plots were used to determine the molecular parameters of large aggregates, which were constructed by plotting $[KC/R_{vv}(q)]^{1/2}$ measured at different concentrations and scattering angles against $(q^2 + kC)$, where k is an arbitrary constant. Extrapolation of $[KC/R_{vv}(q)]^{1/2}$ to zero concentration or angle yields M_w, R_g, and A_2. Figure 10 shows a typical Berry plot for the large $PEEP_{32}$-*b*-$PDMAEMA_{67}$ aggregates at pH 3.0 in deionized water at 22 °C obtained from SLS measurements at scattering angles ranging from 30° to 90° at 10° intervals. From the Berry plot, M_w of the aggregates was about 3.39×10^7 g mol^{-1}, and the aggregation

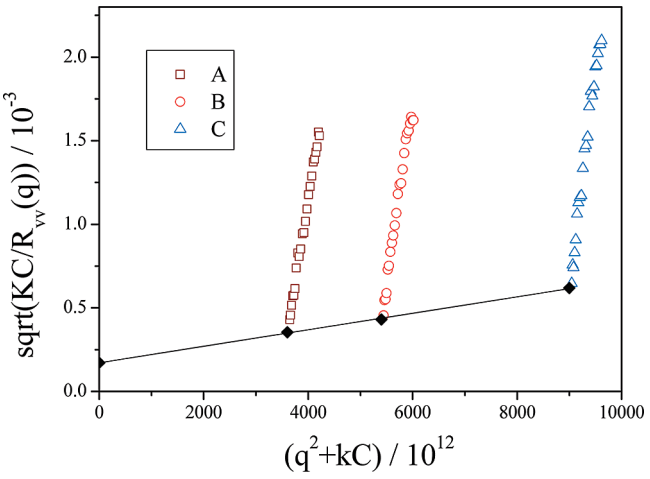

Figure 10. Berry plot of $PEEP_{32}$-*b*-$PDMAEMA_{67}$ aggregates dispersed in water at pH 3.0. The polymer concentration is for (A) 1×10^{-3}, (B) 1.5×10^{-3}, and (C) 2.5×10^{-3} g mL^{-1}.

number N_{agg} was about 1390, since the M_w of a single polymer chain could be determined from ^{1}H NMR (M_n) and GPC measurement of M_w/M_n. This suggests that the microstructure is probably a collection of about 1390 polymer chains. Similarly, the N_{agg} was about 800 at pH 7.4. However, the aggregation number was quite small in basic conditions (pH 10.0) with N_{agg} of about 3, indicating the formation of micelles.

Figure 11 tracked the change of the average particle size as a function of pH values at the polymer concentration of 2.0 g L^{-1}, which was above the cac of $PEEP_{32}$-*b*-$PDMAEMA_{67}$ solution by DLS measurement. From Figure 11a−c (pH 2.93−5.00), the coexistence of large aggregates (about 500 nm) and single polymer chains (about 7 nm) could be obtained from the DLS results. This is because of the different degradation degrees of the polymer chains. A great number of the PEEP-*b*-PDMAEMA block copolymers with negatively charged PEEP block aggregated together into large particles out of the strong electrostatic interactions. And the N_{agg} was 1390, which was much bigger than those formed in both neutral and basic conditions. At the same time, a few undegraded polymers existed in the form of unimers due to the repellence behavior of highly protonated PDMAEMA block. As seen, the number of unimers decreased with the increase of pH values and yielded less degradation. Under neutral conditions (Figure 11d−f, ranged from pH 6 to 8), the hydrolysis of PEEP segments is negligible. Relatively uniformed aggregates of about 300 nm were thus formed due to the interchain entanglements of those randomly distributed short hydrophobic PDMAEMA segments, and the N_{agg} decreased to about 800 at pH 7.4. In contrast, when pH was increased to 9.06 or higher, the PDMAEMA block got fully deprotonated and became hydrophobic; meanwhile, the hydrolysis of PEEP block was accelerated. Thus, the association of PEEP-*b*-PDMAEMA chains was hindered by the repellence of negative charges on hydrolyzed PEEP blocks.[23b] As a consequence, micelles of about 17 nm in size emerged at pH 9.06. Because the degradation rate of main chain was faster than the ethyl groups, the degradation degree, the residue molecular weight, and quantities of negative charge could be varied. And different micelles aggregated together into loosely packed micelles aggregates for this reason. As shown in Figure 11g−i, the number of micelles (17 nm) increased greatly from pH 9.06 to pH 10.98 with an increased degradation degree and the consequent enhanced repellence between PEEP blocks with negative charges.

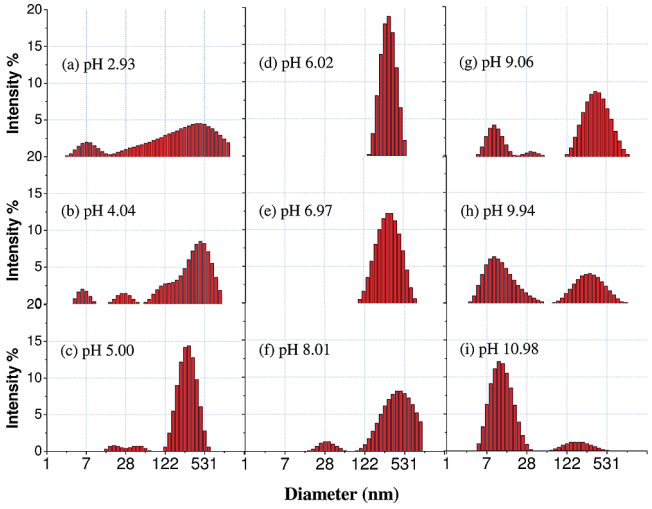

Figure 11. pH-responsive behaviors of aggregates of PEEP-*b*-PDMAEMA at polymer concentration of 2 g L^{-1} in H_2O via DLS measurements at various pH values: (a) pH 2.93, (b) pH 4.04, (c) pH 5, (d) pH 6.02, (e) pH 6.97, (f) pH 8.01, (g) pH 9.06, (h) pH 9.94, and (i) pH 10.98.

Thermal Properties of PEEP-*b*-PDMAEMA Diblock Copolymers. PEEP homopolymer and copolymer with PPEP are thermosensitive with a LCST at around 38 °C or lower.[24] Meanwhile, PDMAEMA exhibits temperature sensitivity resulting from (dimethylamino)ethyl groups and generates the LCST at around 50 °C.[41] In order to determine the dependence of the thermal properties on temperature, the transmittance of light through aqueous solutions of the polymer was measured on a UV-vis spectrometer. The transmittance of 0.5 wt % aqueous solution of the polymers was monitored at 500 nm at a heating or cooling rate of 0.1 °C min^{-1}. We have found that all solutions exhibited a LCST, and their thermoresponsive behaviors were consistently reversible.

Figure 12 shows the repeated temperature dependence of the transmittance of light through $PEEP_{32}$-*b*-$PDMAEMA_{67}$ aqueous solution. The curve coincided well with the variations in temperature regardless of the number of repetitions although hysteresis of change in transmittance between the variations was observed. The phase separation behavior of the copolymer was easily reproducible. At temperatures below the LCST of $PEEP_{32}$-*b*-$PDMAEMA_{67}$ diblock copolymer, the hydrogen bonding between PEEP backbone [−OP(=O)O−] and water molecules is dominant. The PEEP block becomes more hydrophobic with an increase of temperature, which would cause the disruption of hydrogen bonding and dehydration. Therefore, the balance of hydrophilicity and hydrophobicity would shift.[25] Meanwhile, hydrogen bonding formed between (dimethylamino)ethyl groups of PDMAEMA and water molecules can also be disrupted above the LCST, leading to the polymers being hydrophobic and precipitating from the solution.

Figure 13 shows the effect of the composition of the monomer unit on the LCST of the diblock copolymers. The LCST of $PEEP_{32}$-*b*-$PDMAEMA_{31}$ was 66 °C, and it was obvious that LCST of block copolymers decreased when the molecular weight of PDMAEMA increased, while the molecular weight of PEEP block was roughly constant (decreasing from 52 °C of $PEEP_{32}$-*b*-$PDMAEMA_{40}$ to 48 °C of $PEEP_{32}$-*b*-$PDMAEMA_{67}$). In general, the LCST decreases with decreasing hydrophilicity of the polymer.[42] Considering the fact that PDMAEMA block is more hydrophobic compared with PEEP block, it is reasonable that the LCST decreases with

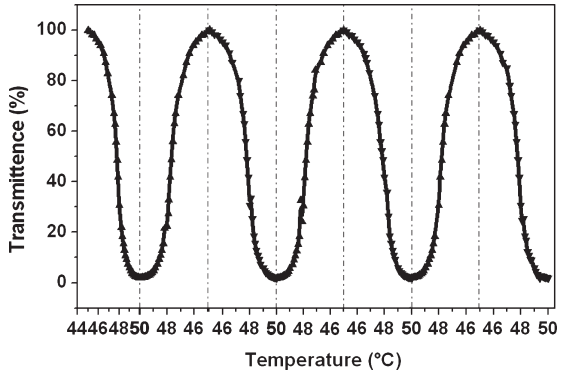

Figure 12. Change in the transmittance of $PEEP_{32}$-*b*-$PDMAEMA_{67}$ polymer solution by repeated thermal cycling.

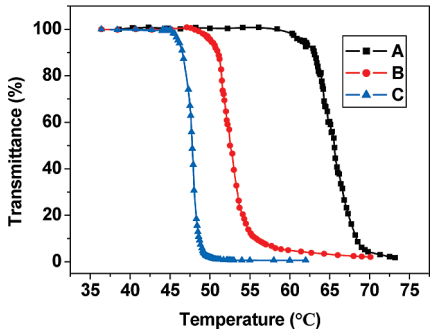

Figure 13. Effects of PDMAEMA lengths on temperature dependence of transmittance changes for 0.5 wt % aqueous solution of PEEP-*b*-PDMAEMA: (A) $PEEP_{32}$-*b*-$PDMAEMA_{31}$; (B) $PEEP_{32}$-*b*-$PDMAEMA_{40}$; (C) $PEEP_{32}$-*b*-$PDMAEMA_{67}$.

the increasing molar fraction of PDMAEMA. Matyjaszewski et al. reported that the LCST of MEO_2MA-*stat*-DMAEMA copolymers increased with the increasing DMAEMA content.[27] In fact, the LCST of thermoresponsive polymers can be controlled by compositions of hydrophobic and hydrophilic units.[43] Thus, LCST can also be further tuned by adjusting the composition of the polyphosphoester block or adding new hydrophobic blocks to find its application under physiological temperatures.

The effect of pH on the thermal properties of $PEEP_{32}$-*b*-$PDMAEMA_{67}$ copolymer was investigated. It showed a sharp decrease in transmittance around their LCST in neutral and basic conditions. The changes, which are summarized in Figure 14, were consistently reversible. The LCST of $PEEP_{32}$-*b*-$PDMAEMA_{67}$ at pH 7.5 was 55 °C. And at pH 8.4, the polymer displayed a lower LCST than that at pH 7.5, suggesting the deprotonation of DMAEMA under basic conditions. Additionally, the LCST of solutions at pH 10 and pH 11 were very close to each other, implying the severe deprotonation of DMAEMA. These results indicate that the PEEP-*b*-PDMAEMA diblock copolymer has been successfully synthesized and possesses pH/temperature-responsive behavior.

Characteristics of Polymer/DNA Complexes. Several research groups have investigated PDMAEMA-PEG copolymers with various architectures in order to address the poor colloidal stabilities of DNA complexes produced by PDMAEMA homopolymers and improve their biological properties.[13,44] Considering PEEP has good biocompatible and biodegradable properties, we used the PEEP-*b*-PDMAEMA diblock copolymer to complex with pDNA because it can offer a potential alternative chemical structure for conferring the necessary steric stabilization and reducing the cytotoxicity.

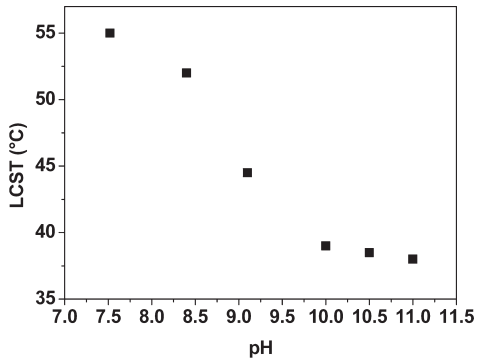

Figure 14. Effect of pH values on LCST of $PEEP_{32}$-*b*-$PDMAEMA_{67}$ (0.5 wt % aqueous solution).

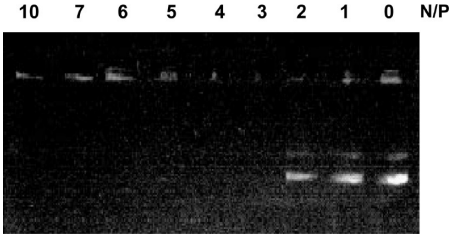

Figure 15. Agarose gel electrophoresis of $PEEP_{32}$-*b*-$PDMAEMA_{67}$/Plasmid pUC 18 DNA complexes at various N/P ratios, as indicated on the top of the lanes. In the panel, the rightmost lane represents the migration of the uncomplexed pUC 18 marker.

One of the prerequisites as a polymeric gene carrier is DNA condensation. Agarose gel retardation electrophoresis was used to study DNA binding affinity of the polymers. We chose $PEEP_{32}$-*b*-$PDMAEMA_{67}$ diblock copolymer as a representative sample for use in the DNA complex. The formation of polyplexes at various N/P ratios was investigated by gel retardation assay, as shown in Figure 15. pDNA was totally retained by the presence of $PEEP_{32}$-*b*-$PDMAEMA_{67}$ at N/P ratio of 3/1 (lane 4). This result revealed that amine groups of PEEP-*b*-PDMAEMA carrying positive charges, which could interact with pDNA phosphate groups with negative charges to form close-neutral complexes. Meanwhile, for PDMAEMA homopolymer of similar molecular weight, complete retardation of free pDNA occurred when the N/P ratio was about 1.0 (date not shown). This phenomenon indicates that the complexation of pDNA with the block copolymers may be partially hindered by the PEEP chains. Similar results have been reported that the PEG segment in block copolymers has interference on their binding affinity to DNA as compared to the homopolymer.[45] An important advantage of PPE over conventionally used PEG is that polyphosphoester is biodegradable, and the degradation rate of polyphosphoester may be adjusted by controlling the chemical structure of the backbone and side chain.

Transport of the gene transfer vector into the target cell is required through different barriers, across the centimeter (in blood circulation) to nanometer size ranges (intracellularly).[46] For efficient endocytosis and gene transfer, the complex must be small (below 150 nm) and compact.[47] Examination

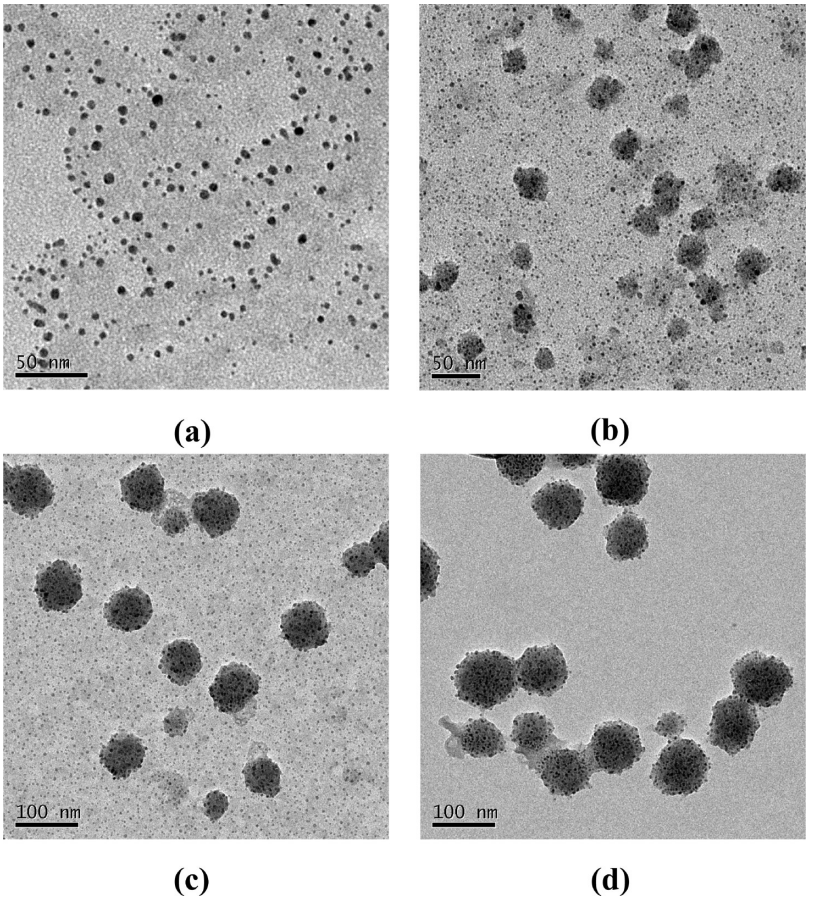

Figure 16. TEM micrographs of various particles formed in 10 mM PBS buffer at pH 7.4: (a) naked DNA particles from Plasmid pUC 18 DNA of 1.0 g L^{-1}, bar = 50 nm; (b) $PEEP_{32}$-*b*-$PDMAEMA_{67}$/pDNA complexes at N/P ratio = 1, bar = 50 nm; (c) $PEEP_{32}$-*b*-$PDMAEMA_{67}$/pDNA complexes at N/P ratio = 2, bar = 100 nm; (d) $PEEP_{32}$-*b*-$PDMAEMA_{67}$/pDNA complexes at N/P ratio = 3, bar = 100 nm.

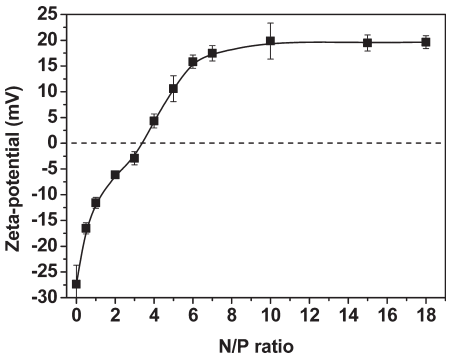

Figure 17. Zeta-potential of $PEEP_{32}$-*b*-$PDMAEMA_{67}$/pDNA complex at various N/P ratios.

of the morphology of the $PEEP_{32}$-*b*-$PDMAEMA_{67}$/pDNA complexes will help us to understand the complex properties and the condensation process. Figure 16 shows the transmission electron microscopy of the naked plasmid DNA and the $PEEP_{32}$-*b*-$PDMAEMA_{67}$/pDNA complexes, which were prepared in PBS buffer at pH 7.4 at various N/P ratios. The images obtained clearly demonstrate significant morphological differences as the N/P ratios were varied. Small and less uniform complexes were formed at lower N/P (1 and 2) with the coexistence of free pDNA molecules that are not engaged in the interaction. Spherical, discrete complexes were achieved at N/P = 3 (mean diameter $\sim$ 95 nm).

Zeta-potential is an indicator of surface charges on the polymer/DNA complexes. A positively charged surface allows electrostatic interaction with anionic cell surfaces and facilitates cellular uptake.[48] The zeta-potential analysis of the $PEEP_{32}$-*b*-$PDMAEMA_{67}$/pDNA complexes were conducted by determining the electrophoretic mobility at 25 °C. Figure 17 showed the zeta-potential changes with various N/P ratios of PEEP-*b*-PDMAEMA/pDNA complexes ranging from 1/2 to 18/1. Naked DNA molecules possessed a negative zeta-potential of −25 mV. The zeta-potential of the resulting complex changed from a negative charge to a positive charge when the amount of $PEEP_{32}$-*b*-$PDMAEMA_{67}$ was increased. When the N/P ratio was higher than 3/1, the surface of pDNA was fully occupied with the PEEP-*b*-PDMAEMA molecules to form positive charge complexes. These results were consistent with the gel retardation electrophoresis data. The PEEP-*b*-PDMAEMA/pDNA complexes carry extra positive charges on their surfaces, which in turn allow better interaction with target cell membrane and therefore an enhanced uptake. From these results, we can conclude that the PEEP-*b*-PDMAEMA diblock copolymer can effectively condense DNA and be used as gene carrier.

Conclusions

In summary, we have utilized the combination of ring-opening polymerization (ROP) and ATRP to synthesize a series of well-defined double-hydrophilic diblock copolymers containing polyphosphoester block and PDMAEMA block. These PEEP-*b*-PDMAEMA diblock copolymers show obvious pH- and temperature-responsive behavior, so they can self-assemble into nanoparticles with different sizes and morphologies when the pH values of aqueous solution were adjusted in the range of 3.0−10. The LCSTs of the diblock copolymers depend on the degrees of polymerization of each block. With the decrease of PDMAEMA units, the increasing LCST can be observed. Besides, PEEP-*b*-PDMAEMA diblock copolymers showed excellent DNA binding characteristics. The PEEP-*b*-PDMAEMA diblock copolymer can effectively condense pDNA at N/P ratio = 3, resulting in small (about 95 nm in size) and positively charged complexes which are suitable for gene delivery. Further modification of the block copolymers and related bioresearch are in progress in our laboratory now. We expect that the polymer would provide potential applications in gene therapy.

Acknowledgment. The authors are thankful for the financial support from the National Natural Science Foundation of China (20974074), the Natural Science Foundation of Jiangsu Province (BK2008157), Qing Lan Project for Innovation Team of Jiangsu Province, and the Program of Innovative Research Team of Soochow University. The authors are indebted to Mr. Weizhong Chen, from University of Science and Technology of China, for his valuable help in LLS experiments and discussion. J.H. has received the financial support from the Innovation Project of Graduate Students of Jiangsu Province, China.

References and Notes

(1) Cölfen, H. *Macromol. Rapid Commun.* **2001**, *22*, 219–252.
(2) Bütün, V.; Liu, S.; Weaver, J. V. M.; Bories-Azeau, X.; Cai, Y.; Armes, S. P. *React. Funct. Polym.* **2006**, *66*, 157–165.
(3) Karanikolopoulos, N.; Pitsikalis, M.; Hadjichristidis, N. Georgikopoulou, K.; Calogeropoulou, T.; Dunlap, J. R. *Langmuir* **2007**, *23*, 4214–4224.
(4) Moore, N. M.; Sheppard, C. L.; Sakiyama-Elbert, S. E. *Acta Biomater.* **2009**, *5*, 854–64.
(5) Uchman, M.; Procházka, K.; Štěpánek, M.; Mountrichas, G.; Pispas, S.; Špírková, M.; Walther, A. *Langmuir* **2008**, *24*, 12017–12025.
(6) Antonietti, M.; Breulmann, M.; Göltner, C. G.; Cölfen, H.; Wong, K. K. W.; Walsh, D.; Mann, S. *Chem.—Eur. J.* **1998**, *4*, 2493–2500.
(7) Cölfen, H.; Antonietti, M. *Langmuir* **1998**, *14*, 582–589.
(8) Guillemet, B.; Faatz, M.; Gröhn, F.; Wegner, G.; Gnanou, Y. *Langmuir* **2006**, *22*, 1875–1879.
(9) Li, Y.; Gong, Y. K.; Nakashima, K.; Murata, Y. *Langmuir* **2002**, *18*, 6727–6729.
(10) Qin, S.; Geng, Y.; Discher, D. E.; Yang, S. *Adv. Mater.* **2006**, *18*, 2905–2909.
(11) Loizou, E.; Triftaridou, A. I.; Georgiou, T. K.; Vamvakaki, M.; Patrickios, C. S. *Biomacromolecules* **2003**, *4*, 1150–1160.
(12) Vihola, H.; Laukkanen, A.; Valtola, L.; Tenhu, H.; Hirvonen, J. *Biomaterials* **2005**, *26*, 3055–3064.
(13) Lin, S.; Du, F.; Wang, Y.; Ji, S.; Liang, D.; Yu, L.; Li, Z. *Biomacromolecules* **2008**, *9*, 109–115.
(14) Wang, J.; Gao, S. J.; Zhang, P. C.; Wang, S.; Mao, M. Q.; Leong, K. W. *Gene Ther.* **2004**, *11*, 1001–1010.
(15) Xiong, M. H.; Wu, J.; Wang, Y. C.; Li, L. S.; Liu, X. B.; Zhang, G. Z.; Yan, L. F.; Wang, J. *Macromolecules* **2009**, *42*, 893–896.
(16) Chaubal, M. V.; Sen Gupta, A.; Lopina, S. T.; Bruley, D. F. *Crit. Rev. Ther. Drug Carrier Syst.* **2003**, *20*, 295–315.
(17) Wang, J.; Zhang, P. C.; Mao, H. Q.; Leong, K. W. *Gene Ther.* **2002**, *9*, 1254–1261.
(18) (a) Zhao, Z.; Wang, J.; Mao, H. Q.; Leong, K. W. *Adv. Drug Delivery Rev.* **2003**, *55*, 483–499. (b) Huang, S. W.; Wang, J.; Zhang, P. C.; Mao, H. Q.; Zhuo, R. X.; Leong, K. W. *Biomacromolecules* **2004**, *5*, 306–311. (c) Lu, Z. Z.; Wu, J.; Sun, T. M.; Ji, J.; Yan, L. F.; Wang, J. *Biomaterials* **2008**, *29*, 733–741. (d) Iwasaki, Y.; Akiyoshi, K. *Biomacromolecules* **2006**, *7*, 1433–1438.
(19) Xu, X.; Yu, H.; Gao, S.; Mao, H. Q.; Leong, K. W.; Wang, S. *Biomaterials* **2002**, *23*, 3765–3772.
(20) Li, Q.; Wang, J.; Shahani, S.; Sun, D. D. N.; Sharma, B.; Elisseeff, J. H.; Leong, K. W. *Biomaterials* **2006**, *27*, 1027–1034.
(21) Wen, J.; Kim, G. J. A.; Leong, K. W. *J. Controlled Release* **2003**, *92*, 39–48.
(22) Yang, X. Z.; Wang, Y. C.; Tang, L. Y.; Xia, H.; Wang, J. *J. Polym. Sci., Part A: Polym. Chem.* **2008**, *46*, 6425–6434.
(23) (a) Chen, D. P.; Wang, J. *Macromolecules* **2006**, *39*, 473–475. (b) Wang, Y. C.; Tang, L. Y.; Sun, T. M.; Li, C. H.; Xiong, M. H.; Wang, J. *Biomacromolecules* **2008**, *9*, 388–395. (c) Wang, Y. C.; Liu, X. Q.; Sun, T. M.; Xiong, M. H.; Wang, J. *J. Controlled Release* **2008**, *128*, 32–40. (d) Cheng, J.; Ding, J. X.; Wang, Y. C.; Wang, J. *Polymer* **2008**, *49*, 4784–4790. (e) Yuan, Y. Y.; Wang, Y. C.; Du, J. Z.; Wang, J. *Macromolecules* **2008**, *41*, 8620–8625.
(24) Iwasaki, Y.; Wachiralarpphaithoon, C.; Akiyoshi, K. *Macromolecules* **2007**, *40*, 8136–8138.

(25) Wang, Y. C.; Tang, L. Y.; Li, Y.; Wang, J. *Biomacromolecules* **2009**, *10*, 66–73.
(26) Liu, F.; Urban, M. W. *Macromolecules* **2008**, *41*, 6531–6539.
(27) Yamamoto, S.; Pietrasik, J.; Matyjaszewski, K. *Macromolecules* **2008**, *41*, 7013–7020.
(28) (a) van de Wetering, P.; Cherng, J. Y.; Talsma, H.; Crommelin, D. J. A.; Hennink, W. E. *J. Controlled Release* **1998**, *53*, 145–153. (b) van de Wetering, P.; Cherng, J. Y.; Talsma, H.; Hennink, W. E. *J. Controlled Release* **1997**, *49*, 59–69. (c) Jones, R. A.; Poniris, M. H.; Wilson, M. R. *J. Controlled Release* **2004**, *96*, 379–391.
(29) Libiszowski, J. K. K.; Penezek, S. *J. Polym. Sci., Polym. Chem. Ed.* **1978**, *16*, 1275–1283.
(30) Jakubowski, W.; Lutz, J. F.; Slomkowski, S.; Matyjaszewski, K. *J. Polym. Sci., Part A: Polym. Chem.* **2005**, *43*, 1498–1510.
(31) Chu, B. *Laser Light Scattering*, 2nd ed.; Academic Press: New York, 1991.
(32) Wu, C.; Xia, K. Q. *Rev. Sci. Instrum.* **1994**, *65*, 587–590.
(33) Xiao, C. S.; Wang, Y. C.; Du, J. Z.; Chen, X. S.; Wang, J. *Macromolecules* **2006**, *39*, 6825–6831.
(34) Mao, B. W.; Gan, L. H.; Gan, Y. Y.; Li, X.; Ravi, P.; Tam, K. C. *J. Polym. Sci., Part A: Polym. Chem.* **2004**, *42*, 5161–5169.
(35) Moller, M. A.; Augenstein, M.; Durmont, E.; Pennewiss, H. *New Polym. Mater.* **1991**, *2*, 315–329.
(36) Kalyanasundaram, K.; Thomas, J. K. *J. Am. Chem. Soc.* **1977**, *99*, 2039–2044.
(37) Tan, J. F.; Ravi, P.; Too, H. P.; Hatton, T. A.; Tam, K. C. *Biomacromolecules* **2005**, *6*, 498–506.
(38) Baran, J.; Penczek, S. *Macromolecules* **1995**, *28*, 5167–5176.
(39) Sfika, V.; Tsitsilianis, C. *Macromolecules* **2003**, *36*, 4983–4988.
(40) Plunkett, K. N.; Moore, J. S. *Langmuir* **2004**, *20*, 6535–6537.
(41) Yuk, S. H.; Cho, S. H.; Lee, S. H. *Macromolecules* **1997**, *30*, 6856–6859.
(42) Feil, H.; Bae, Y. H.; Feijen, J.; Kim, S. W. *Macromolecules* **1993**, *26*, 2496–2500.
(43) Tachibana, Y.; Kurisawa, M.; Uyama, H.; Kakuchi, T.; Kobayashi, S. *Chem. Commun.* **2003**, 106–107.
(44) Rungsardthong, U.; Deshpande, M.; Bailey, L.; Vamvakaki, M.; Armes, S. P.; Garnett, M. C.; Stolnik, S. *J. Controlled Release* **2001**, *73*, 359–380.
(45) Petersen, H.; Fechner, P. M.; Martin, A. L.; Kunath, K.; Stolnik, S.; Roberts, C. J.; Fischer, D.; Davies, M. C.; Kissel, T. *Bioconjugate Chem.* **2002**, *13*, 845–854.
(46) Kostarelos, K. *Adv. Colloid Interface Sci.* **2003**, *106*, 147–168.
(47) Liu, G.; Molas, M.; Grossmann, G. A.; Pasumarthy, M.; Perales, J. C.; Cooper, M. J.; Hanson, R. W. *J. Biol. Chem.* **2001**, *276*, 34379–34387.
(48) Zauner, W.; Ogris, M.; Wagner, E. *Adv. Drug Delivery Rev.* **1998**, *30*, 97–113.